Molecular mechanism of pyroptosis of mononuclear macrophages induced by pathogenic E. coli high pathogenicity island (HPI) in Yunnan Saba pigs

Chunlan Shan
Yunnan Agricultural University
Shushu Miao
Yunnan Agricultural University
Chaoying Liu
Yunnan Agricultural University
Weiwei Zhao
Yunnan Agricultural University
Bo Zhang
Yunnan Agricultural University
Wei Yang
Yunnan Agricultural University
Hao Wang
Yunnan Agricultural University
Jinlong Cha
Yunnan Agricultural University
Ru Zhao
Yunnan Agricultural University
Libo Gao
Yunnan Agricultural University
Hong Gao (gaohongping@163.com)

Research

Keywords: Pathogenic E. coli, HPI, Mononuclear macrophage, Pyroptosis

Posted Date: February 27th, 2020

DOI: https://doi.org/10.21203/rs.2.24631/v1

Molecular mechanism of pyroptosis of mononuclear macrophages induced by pathogenic *E. coli* high pathogenicity island (HPI) in Yunnan Saba pigs

Chunlan Shan[a,1], Shushu Miao[b,1], Chaoying Liu[a] , Weiwei Zhao[c] , Bo Zhang[a] , Wei Yang[b] , Hao Wang[b] , Jinlong Cha[b] , Ru Zhao[b] , Libo Gao[b] , Hong Gao[b,*]

[a] College of Animal Science and Technology, Yunnan Agricultural University, 650201, Kunming, China

[b] College of Veterinary Medicine, Yunnan Agricultural University, 650201, Kunming, China

[c] College of Food Science and Technology, Yunnan Agricultural University, 650201, Kunming, China

***Corresponding author:**

Hong Gao, College of Veterinary Medicine, Yunnan Agricultural University, Kunming, 650201, P.R China. E-mail: gaohongping@163.com

1 These authors contributed equally to this work.

Abstract

Background

In this study we evaluated the molecular mechanism by which pyroptosis is induced in mononuclear macrophages isolated from Saba pigs following infection with pathogenic *E. coli* high pathogenicity island (HPI). Mononuclear macrophages were divided into four treatment groups: control, Lipopolysaccharide (LPS) + adenosine triphosphate (ATP), HPI positive (+) strain and HPI negative (-) strain. The mononuclear macrophages and their culture supernatants were collected at 0.5, 3, 6, 9, 12 and 24 h after infection. DNA changes were detected by TUNEL staining and the integrity of the cell membrane was evaluated by propidium iodide (PI) staining. Changes in mRNA expression levels of NLRP3, caspase-1, IL-1β, and IL-18 gene in mononuclear macrophages were analyzed by quantitative real-time polymerase chain reaction (RT-PCR) and caspase-1 protein expression was detected by indirect immunofluorescence. IL-1β and IL-18 concentration in the mononuclear macrophage culture supernatant were measured by ELISA.

Results

Compared with the control group, TUNEL and PI staining of mononuclear macrophages was significantly increased following infection with the HPI^+/HPI^- strains ($P < 0.01$ or $P < 0.05$), with significantly higher levels detected in the HPI^+ group compared with those in the HPI^- group ($P < 0.01$ and $P<0.05$). Compared with the control group, the expression levels of NLRP3, caspase-1, IL-1β, and IL-18 in the HPI groups were upregulated after pathogenic *E. coli* infection, with significantly higher levels detected in the HPI^+ group compared with those in the HPI^- group ($P < 0.01$ or $P < 0.05$).

Conclusions

These findings showed that pathogenic *E. coli* HPI infection of Saba pigs results induced pyroptosis of mononuclear macrophages characterized by increased expression of NLRP3,

caspase-1, IL-1β and IL-18 mRNA in mononuclear macrophages, the induction of cell membrane pore formation, nuclear DNA damage, and the secretion of IL-1β and IL-18 to enhance the inflammatory response.

Key words: Pathogenic *E. coli*; HPI; Mononuclear macrophage; Pyroptosis

Background

Escherichia coli (*E. coli*), which is a typical Gram-negative member of the coliform genus *Escherichia*, plays an important role in the intestinal symbiosis of warm-blooded animals [1, 2]. Pathogenic *E. coli* strains cause serious harm to human and animal health, often causing severe diarrhea edema and septicemia [3]. High pathogenicity island (HPI) is an important factor for the virulence and pathogenicity of *E. coli*, and other highly pathogenic strains. It was first discovered in *Yersinia* [4] and is present only in virulent strains [5]. HPI has a functional core region, containing the *irp2-irp1-irp3-irp4-irp5-FyuA* gene axis known as the *irp2-FyuA* gene cluster, and the *irp2* marker gene [6]. Paauw et al. demonstrated that *Yersinia* containing HPI was more virulent by studying the iron carrier encoding HPI [7].

Inflammatory caspases such as caspase-1 (mouse/human), caspase-4 (human), and caspase-11 (mouse), contribute to a variety of biological functions [8, 9]. Pyroptosis is a form of programmed cell death mediated by a caspase-1, which induces cell swelling and is characterized by the rupture and release of cellular contents leading to an intense inflammatory reaction that is essential for the control of microbial infections [10].

Nucleotide-binding oligomerization domain-like receptor family pyrin domain-containing 3(NLRP3) inflammasomes are mainly composed of intracellular pattern-recognition receptor NLRP3, adaptor protein ASC, and pro-caspase-1 [11]. The NLRP3 inflammasome is involved in the regulation of immune responses, and can be activated by bacteria, viruses, fungi and apoptosis [12]. NLRP3 inflammasomes activate the caspase-1 domain. The activated caspase-1 then cleaves inactive pro-interleukin-1β (pro-IL-1β) and pro-interleukin-18 (pro-IL-18) to generate the active pro-inflammatory cytokines IL-1β and IL-18 [13].

Activated caspase-1 and its precursors cleave gasdermin D (GSDMD) protein to separate its N-terminal domain from its C-terminal domain, which relieves the inhibition of

the N-terminal domain by the C-terminal domain of the GSDMD protein [14]. After cleavage, the N-terminal domain of the GSDMD protein binds to phosphatidylinositol on the cytoplasmic membrane, oligomerizes on the cytoplasmic membrane and forms membrane pores with an inner diameter of 12-14 nm [14]. During pyroptosis, specific pores are formed on the cell membrane of the target cell, resulting in disruption of the ion concentration gradient across the cell membrane, and leading to the swelling and disintegration of the cells [15-17]. Mature IL-1β and IL-18 are then released from the cytoplasm through this cell membrane pore [14]. Other immune cells are recruited and stimulated by IL-1β and IL-18, thereby inducing the synthesis of other inflammatory cytokines and enhancing the local and systemic inflammatory response [18].

Several characteristics of pyroptosis appear to overlap with apoptosis, although the process are distinct. Similar to apoptosis, cells incur DNA damage during pyroptosis [19], and become positive in the TUNEL assay [20-22]. In contrast, the nuclear morphology of pyroptotic cells is distinct from that of apoptotic cells [21], and a DNA ladder is not necessarily observed [22].

It has been confirmed that *Shigella flexneri*, *Salmonella*, *Listeria*, *Pseudomonas aeruginosa*, *Francis tularensis*, *Legionella pneumophila* and *Yersinia* induce caspase-1-dependent pyroptosis in macrophages [18]. During infection, pyroptosis induces the death of host cells, which is an important process by which the growth and reproduction of the pathogenic microorganism is limited and the infection is cleared, thus providing effectively protection of the host. Miao et al. reported that caspase-1 gene knockout mice were resistant to the death induced by *Salmonella typhimurium*, indicating the importance of caspase-1 in resisting pathogen invasion [23].

Pyroptosis is closely related to the control of various bacterial infectious diseases; however, its mechanism and regulation mechanism has not been elucidated. Saba pigs are a

breed local to Yunnan Province that are reared for their high rate of piglet production and an excellent meat quality. Saga sows are commonly used in hybrid breeding systems in central Yunnan Province [24].

To elucidate the pathogenic mechanism of *E. coli*, we evaluated the ability of pathogenic *E. coli* HPI to induce pyroptosis in mononuclear macrophages, and investigated the underlying mechanism. In addition, we explored the effects of HPI^+ and HPI^- strains on host cell infection. This information will provide a better understanding of the mechanism of pyroptosis-related diseases, and highlight new therapeutic targets for the treatment of related diseases.

Result

Isolation and identification of pathogenic E. coli HPI

The *E. coli* HPI strains were cultured for 24 h until bright pink round colonies with smooth and moist surface and flat, neat edges were observed (Fig. 1A). Translucent raised colonies that were round in shape and with a smooth, moist surface were formed on normal nutrient agar medium (Fig. 1B). *E.coli* were identified as Gram-positive rod-shaped red cells (Fig. 1C). The presence of the *irp2* gene in the isolates was determined by PCR amplification using the extracted DNA as a template. In total, 43 of the 96 isolates were *irp2* gene positive (44.8%) and 53 were negative (55.2%). Representative results for PCR amplification of the HPI *irp2* gene are shown in Figure 1D.

MTT analysis of cell viability

The IC_{50} for LPS was calculated to be approximately 10 μg/ mL according to the Improved Kou method (Figure 2).

TUNEL detection

As shown in Figure 3A and B, the IOD values representing the intensity of TUNEL staining of the experimental groups was significantly higher than that of the control group during the period from 0.5 to 9 h post-infection ($P < 0.01$). The IOD value of the LPS+ATP group was significantly higher than that of the other groups after infection ($P < 0.01$). The IOD values in the HPI treated groups were significantly higher than those in the control group at 0.5 and 3 h post-infection ($P < 0.01$). As the bacteria multiplied, the IOD value of the HPI^+ group was obviously different than that of the HPI^- group at 9 h post-infection ($P < 0.01$).

PI staining

As shown in Figure 4A and B, the IOD values representing the intensity of PI staining of the HPI groups were significantly higher than that of the control group during the period of 0.5 to 9 h post-infection ($P < 0.01$). The IOD value of the LPS+ATP group was significantly higher than those in the other groups after infection ($P < 0.01$). The IOD values of the HPI^+ group were markedly higher than those of the HPI^- at different time-points after *E. coli* infection, with significant differences detected at 0.5 and 9 h ($P < 0.05$) and extremely significant differences detected at 3 h ($P < 0.01$).

Effects of HPI infection on the mRNA expression of key pyroptosis genes in mononuclear macrophages

As shown in Figure 5A, NLRP3 mRNA expression in the experimental groups was significantly higher than that in the control group at 0.5, 3 and 6 h post-infection ($P < 0.01$). In addition, NLRP3 mRNA expression in the HPI^+ group was significantly higher than that in the HPI^- and control groups at 24 h post-infection ($P < 0.01$).

As shown in Figure 5B, the relative expression of caspase-1 mRNA in the experimental

groups was higher than that in the control group after *E. coli* infection, with significant differences between the HPI treatment and control groups at 3, 6, 9, 12 and 24 h ($P < 0.01$). At each time-point after infection, caspase-1 expression in the HPI^+ group was significantly higher than that in the HPI^- group ($P < 0.01$), while the caspase-1 expression level in the HPI^+ group was significantly lower than in the LPS+APS group at 3 and 6 h ($P < 0.01$).

As shown in Figure 5C and D, the relative mRNA expression of IL-1β and IL-18 in the experimental groups was higher than that in the control group at 6, 9 and 12 h post-infection. The IL-1β and IL-18 expression levels in the HPI^+ group were significantly different from those in the control group after infection ($P < 0.01$ or $P < 0.05$). The IL-1β expression levels in the HPI^+ group were significantly higher than those in the HPI^- group and control group at 6 and 9 h post-infection ($P < 0.01$). The IL-18 expression levels in the HPI^+ group were significantly higher than those in the control group at 6, 9 and 12 h post-infection ($P < 0.01$), and were significantly higher than those in the HPI^- at all time-points except 6 h ($P < 0.01$). Additionally, with increasing time after infection, the relative mRNA expression of IL-1β and IL-18 gradually increased in the HPI groups.

Immunofluorence assay (IFA) of caspase-1 protein expression in mononuclear macrophages

As shown in Figures 6A and B, the IOD values representing the intensity of caspase-1 protein staining in the experimental groups increased during the period from 0.5 to 9 h post-infection. However, at 0.5 h post-infection, the IOD values of caspase-1 protein in the experimental groups were significantly decreased compared with those in the control group ($P < 0.01$), while those in the HPI^+ group were significantly higher than those in the HPI^- group ($P < 0.01$). At 3 and 9 h post-infection, the IOD values of caspase-1 protein in the experimental groups were significantly higher than those in the control group ($P < 0.01$). Furthermore, the

IOD values of caspase-1 protein in the HPI^+ group were significantly higher than those in the HPI^- ($P < 0.01$).

ELISA analysis of IL-1β and IL-18 levels in mononuclear macrophages after E. coli infection

The concentrations of IL-1β and IL-18 in the culture supernatants of mononuclear macrophages were detected by ELISA (Fig. 7A and B). The concentrations both cytokines increased gradually with time after infection. The IL-1β content in the LPS+ATP group was significantly higher than that in the control group at 0.5, 3, 6 and 24 h post-infection ($P < 0.01$ or $P < 0.05$). The IL-1β content in the HPI^+ group was significantly higher than that in the control group at 3, 6, 12 and 24 h post-infection ($P < 0.05$), whereas the difference were not statistically significant at the other time-points ($P > 0.05$). The IL-1β content in the HPI^- group was significantly higher than that in the control group at 3 h post-infection ($P < 0.05$). The IL-18 content in the control group was significantly lower than those in the experiment groups at 6 and 24 h post-infection ($P < 0.01$, $P < 0.05$ or $P > 0.05$). The IL-18 content in the LPS+ATP group was significantly higher than the other groups at 0.5, 3, 9 and 12 h post-infection ($P < 0.05$ or $P > 0.05$). The IL-18 content in the HPI^+ group was significantly higher than that in the HPI^- group at 6 h post-infection ($P < 0.05$).

Discussion

Pyroptosis is a form of innate immune defense against intracellular bacteria [23]. This type of programmed cell death is accompanied by an inflammatory response that induces both apoptosis and necrosis, which are characterized by DNA and membrane damage. Similar to apoptosis, the chromatin DNA in pyroptotic cells is damaged and broken, rendering TUNEL staining-positive [25]. However, in contrast to apoptosis, numerous pores (1–2 nm) are

formed on the cell membrane of pyroptotic cells, leading to the release of the cellular contents and inflammatory factors, such as IL-1β, which further promote the inflammatory response [26]. Studies have shown that when cells undergo pyroptosis, PI can cross the pores in the cell membrane to stain the nucleus red [27]. Fink et al. reported that *Salmonella* infection of mice caused pyroptosis of host macrophages, with the formation of membrane pores (1.1–2.4 nm) causing cell swelling due to disruption of the osmotic gradient [28]. In this study, after infection of mononuclear macrophages with pathogenic *E. coli* HPI, the IOD value of PI staining was significantly increased, with higher values in the HPI^+ treatment group than that in the HPI^-. This indicated that *E. coli* HPI infection promoted the formation of pores in the cell membrane of mononuclear macrophages, and this effect was more marked in the presence of the HPI *irp2* gene. This is consistent with the observation that the number of PI-positive macrophages increased with time after infection with listeria [29].

Muruve and Lamkanfi observed clear signs of pyroptosis and marked increases in the relative mRNA levels of NLRP3, caspase-1, IL-1β and IL-18 after LPS/ATP stimulation of mouse macrophages [30, 31]. Liang reported that the mRNA expression levels of pyroptosis-related genes (NLRP3, caspase-1, IL-1β and IL-18) were significantly increased in renal tissues after obstructive nephropathy caused by unilateral ureteral ligation in rats [32]. In this study, after pathogenic *E. coli* infection of mononuclear macrophages in vitro, the intracellular mRNA expression levels of NLRP3, caspase-1, IL-1β and IL-18 were higher than those in the control group, with an overall increase in levels observed initially followed by decreased expression, which was consistent with previous reports. The findings indicate that *E. coli* activates the pyroptosis signaling pathway, and this effect is promoted more effectively by *E. coli* HPI. In this study, caspase-1 protein expression varied with the different treatments. Caspase-1 protein expression in the LPS+ATP group and the HPI groups increased gradually with time post-infection, which is similar to the pattern of increased

caspase-1 protein content in human monocyte macrophages following *Helicobacter pylori* infection [33]. Furthermore, it has been reported that *Neisseria gonorrhoeae* infection promoted the activation and secretion of caspase-1 in human monocytes [34]. Our study confirmed that pathogenic *E. coli* HPI induces pyroptosis in monocyte macrophages, and caspase-1 protein expression was higher in host cells infected HPI^+ strains containing the HPI *irp2* marker gene.

IL-1β and IL-18 are belong to IL-1 family and are produced by monocyte endothelial cell fibroblasts and other cell types in response to infection. These cytokines play an inflammatory role by binding to the corresponding receptors to regulate the release of soluble antagonists and the expression of precursor enzymes and bait receptors at the transcriptional level. In addition, they also participate in congenital and adaptive immune effector cells of the recruitment and activation. IL-1β and IL-18 are synthesized as inactive cytoplasmic (pro-IL-1β and pro-IL-18) and maturation depends on the caspase-1 activity [35]. The mature forms of IL-1β and IL-18 are released through the GSDMD channel to perform their pro-inflammatory functions and cause pyroptosis [30]. Hitzler showed that *H. pylori* infection of dendritic cells resulted in activation of caspase-1 and induced the maturation and secretion of IL-1β and IL-18 [36].

The results of our study demonstrated that IL-1β/IL-18 levels were significantly elevated in the culture supernatants of mononuclear macrophages infected with *E.coli* HPI, with higher levels detected following infection with the strain carrying the *irp2* gene. These findings provide evidence of the initial activation of the NLRP3/caspase-1 pyroptosis pathway in cells following HPI infection, which further promoted the secretion of inflammatory inflammatory factors IL-1β and IL-18. This is consistent with the significant increase in IL-1β and IL-18 expression after LPS/ATP stimulation of mouse macrophages reported by Wei [37]. These findings effectively confirm that HPI endows characteristics of

strong pathogenicity on *E.coli*, which is closely related to the process of infection.

Conclusion

In conclusion, we found that pathogenic *E.coli* HPI infection of Yunnan Saba pigs upregulated the expression of NLRP3, caspase-1, IL-1β and IL-18 mRNA, and promoted cell membrane pore formation and nuclear DNA damage in mononuclear macrophages. Furthermore, we showed that the infection stimulated the release of inflammatory cytokines IL-1β and IL-18, induce inflammation, and eventually promoted pyroptosis of mononuclear macrophages. Moreover, the existence of HPI in *E.coli* enhanced the occurrence of pyroptosis of mononuclear macrophages compared with the effects observed following infection with the HPI^- strain. The correlation of *E.coli* HPI infection with the expression of key pyroptosis-related molecules in monocytes highlights new ideas and directions for further studies to elucidate the molecular mechanism by which *E.coli* HPI induces pyroptosis in mononuclear macrophages. Further studies of pyroptosis will contribute to a greater understanding of the mechanisms of cellular injury and to the development of pharmaceutical inhibitors of pyroptosis.

Materials and methods

Materials and reagents

Mononuclear macrophages were isolated from the peripheral blood of four healthy slag pigs (2 boars and 2 sows) aged 1–4 months. HPI^+ and HPI^- strains of pathogenic *E.coli* were isolated at the laboratory of a pig farm in Chuxiong City, Yunnan Province (China), identified and preserved by the department of animal pathology (Yunnan Agricultural University) [38]. The HPI gene of *E.coli* was identified by polymerase chain reaction (PCR). HPI^+ and HPI^-

strains have the same serotype (O119) and biochemical characteristics which were tested by the method reported by Jing et al. [39]. Chloroform and alcohol concentration gradients were from Beijing Chemical Industry Group Co., Ltd. (Beijing, China).

PCR detection of HPI irp2 gene and culture of mononuclear macrophages

The *E. coli* HPI strains isolated from Saba pigs were cultured on MacConkey agar medium at 37℃ for 24 h. Individual colonies of pathogenic *E.coli* were selected, inoculated and cultured on Luria-Bertani (LB) agar plates overnight at 37℃. At OD_{600} 0.6–0.8, bacterial suspensions (containing HPI^+/ HPI^-), expression of the HPI *irp2* genes was analyzed by PCR using the *irp2* primers shown in Table 1. The PCR conditions were as follows: 95°C for 5 min; 94°C for 30 s, 55°C for 30 s, 72°C for 1 min (32 cycles) and one final extension step of 72°C for10 min. The PCR products were resolved by 1.0% (wt/vol) agarose gel electrophoresis.

Mononuclear macrophages were cultured in DMEM containing 10% FBS, penicillin and streptomycin at 37℃ under 5% CO_2.

MTT assay of cell viability

Cells in the control and the experimental groups seeded into 96-well plates at 2×10^5/well with five duplicate wells for each group. Medium (100 μL) containing different concentrations of LPS (10^6, 10^5, 10^4, 10^3, 10^2 and 10 ng/mL) was added to each well. After 5.5 h, 10 μL ATP (55 mmol/L) was added. After 24 h, 10 μL MTT reagent (5 mg/mL) was added to each well. After a further 4 h, the culture supernatant was removed and 100 μL DMSO was added to each well. The plate was oscillated for 15 min before the absorbance at 490 nm was measured using an ELx800™ Absorbance Microplate Reader (BioTek Instruments, Winooski, USA). The IC_{50} for LPS was calculated according to the Improved Kou method, where $lgIC_{50}$ = Xm-I(P-(3-Pm-Pn)/4). Xm:lg maximum dose; I:lg(maximum dose/ phase dose); P: sum of

positive response rates; Pm: maximum positive response rate; Pn: minimum positive response rate.

Mononuclear macrophages infected with E. coli

The mononuclear macrophages were randomly divided into four groups: control, HPI^+ infection, HPI^- infection and LPS+ATP, with three replicates for each group. Mononuclear macrophages were seeded in 96-well plates at 2×10^5/well and infected with HPI^+ strains, HPI^- strains, and LPS+ATP by adding 2 mL of cell culture broth containing 1 mL of bacterial suspension (OD_{600} 0.6–0.8). At 0.5, 3, 6, 9, 12 and 24 h post-infection, mononuclear macrophages and their supernatant were collected for analysis.

Real-time polymerase chain reaction (RT-PCR)

Total RNA was extracted, cDNA was synthesized by reverse transcription and stored at −20° C. RT-PCR reverse transcription kits and SYBR Premix Ex TaqTM II were purchased from TaKaRa Biotechnology Co., Ltd. (Dalian, China). The RT-PCR reaction was carried out using gene-specific primers for β-actin, NLRP3, caspase-1, IL-1β and IL-18 (Table 1). The amplification was carried out using the Bio-Rad Cx96 Detection System under the following reaction conditions: 95°C 30 s; 95°C 5 s, Tm 47–62°C 20 s, 72°C 30 s (40 cycles). The relative mRNA expression for each index was calculated using the $2^{-\triangle\triangle Ct}$ method.

TUNEL detection

Cells were prepared as described in section 2.4. Cells were seeded in 6-well plates (2×10^6/well) and fixed with 4% paraformaldehyde on ice for 15 min. The supernatant was centrifuged and fixed in 70% cold ethanol for 24 h. TUNEL staining was then performed using TUNEL kits (R&D Systems Co. Ltd., Shanghai, China) according to the

manufacturer's instructions.

Propidium iodide (PI) staining

Cells were prepared as described in section 2.4. Cells were seeded in 96-well plates (2×10^5/well), with three replicates for each group. The cells were cultured with 100 μL of 6.7 μg/mL PI staining solution at 37℃ for 20 min. Mononuclear macrophages were observed under a light microscope at 200× amplification (Olympus IX73P1F microscope, Japan)

Immunofluorence assay (IFA) of HPI on caspase-1 protein expression into mononuclear macrophages

Cells were prepared as described in section 2.4. Cells were fixed, permeabilized and then incubated overnight at 4℃ with anti-caspase-1 (1:50, mouse monoclonal, Santa Cruz Biotechnology USA). The cells were then incubated in the dark with secondary detection antibodies before 4', 6-diamidino-2-phenylindole (DAPI) treatment. The IOD values for caspase-1 protein expression were analyzed using Image Pro-Plus 6.0 software (Media Cybernetics, Silver Spring, MD, USA).

ELISA

Cells were prepared as described in section 2.4. The supernatants from cells in each group were collected and the contents of the inflammatory mediators IL-1β and IL-18 were detected by commercially available Porcine IL-1β and IL-18 ELISA kits (Shanghai Yuanye Biotechnology Co. Ltd., Shanghai, China) according to the manufacturers' instructions.

Statistical analysis

All data were presented as the mean ± SD (n = 3), and significance of differences between

groups were evaluated by ANOVA, followed by the Duncan post-hoc test. Differences were regarded as significant and highly significant at $P < 0.05$ and $P < 0.01$, respectively.

Declarations

Ethics approval and consent to participate

All methods were non-invasive and were approved by the Committee on the Ethics of Animal Experiments of the Yunnan Agricultural University.

Consent for publication

All authors have approved this submitted manuscript in its current form and agreed to publish.

Availability of data and materials

The data sets generated in the current study are available from the corresponding author on reasonable request.

Competing interests

All authors declare that they have no conflict of interests.

Funding

This study was supported by the National Natural Science Foundation of China (Grant Nos. 31660704 and 31960692).

Authors' contributions

Chunlan Shan and Shushu Miao contributed equally to this work.

Affiliations

College of Animal Science and Technology, Yunnan Agricultural University, Kunming, P.R China.

Chunlan Shan, Chaoying Liu, Bo Zhang

Department of Animal Pathology, College of Veterinary Medicine, Yunnan Agricultural University, Kunming, P.R China.

Shushu Miao, Wei Yang , Hao Wang , Hong Gao , Ru Zhao , Libo Gao

College of Food Science and Technology, Yunnan Agricultural University, Kunming, P.R China.

Weiwei Zhao

Contributions

Chunlan Shan and Shushu Miao designed and supervised the study, reviewed and edited the manuscript. All authors read and approved the final manuscript.

Corresponding author

Correspondence to Hong Gao, College of Veterinary Medicine, Yunnan Agricultural University, Kunming, P.R China.

Acknowledgements

This work was financially supported by the National Natural Science Foundation of China (Grant No. 31660704; 31960692). We are grateful to all other staff at Yunnan Agricultural University for their assistance with the experiments.

References

1. Stromberg ZR, Johnson JR, Fairbrother JM, Kilbourne J, Van Goor A, Curtiss RR, et al. Evaluation of Escherichia coli isolates from healthy chickens to determine their potential risk to poultry and human health. PLoS ONE. 2017; 12(7):e0180599-e. doi:10.1371/journal.pone.0180599.
2. Croxen MA, Law RJ, Scholz R, Keeney KM, Wlodarska M, Finlay BB. Recent advances in understanding enteric pathogenic Escherichia coli. Clin Microbiol Rev. 2013; 26(4):822-80. doi:10.1128/CMR.00022-13.
3. Makvana S, Krilov LR. Escherichia coli Infections. Pediatr Rev. 2015; 36(4):167-71. doi:10.1542/pir.36-4-167.
4. Mokracka J, Koczura R, Kaznowski A. Yersiniabactin and other siderophores produced by clinical isolates ofEnterobacterspp. andCitrobacterspp. FEMS Immunol Med Microbiol. 2004; 40(1):51-5. doi:10.1016/s0928-8244(03)00276-1.
5. Hacker J, Blum-Oehler G, Muhldorfer I, Tschape H. Pathogenicity islands of virulent bacteria: structure, function and impact on microbial evolution. Molecular Microbiology. 1997; 23(6):1089-97. doi:10.1046/j.1365-2958.1997.3101672.x.
6. Schouler C, Schaeffer B, Brée A, Mora A, Dahbi G, Biet F, et al. Diagnostic strategy for identifying avian pathogenic Escherichia coli based on four patterns of virulence genes. Journal of clinical microbiology. 2012; 50(5):1673-8. doi:10.1128/JCM.05057-11.
7. Paauw A, Leverstein-van Hall MA, van Kessel KPM, Verhoef J, Fluit AC. Yersiniabactin reduces the respiratory oxidative stress response of innate immune cells. PLoS ONE. 2009; 4(12):e8240-e. doi:10.1371/journal.pone.0008240.
8. Martinon F, Tschopp J. Inflammatory Caspases. Cell. 2004; 117(5):561-74. doi:10.1016/j.cell.2004.05.004.
9. Man SM, Kanneganti T-D. Converging roles of caspases in inflammasome activation,

cell death and innate immunity. Nat Rev Immunol. 2016; 16(1):7-21. doi:10.1038/nri.2015.7.

10. Xia X, Wang X, Zheng Y, Jiang J, Hu J. What role does pyroptosis play in microbial infection? Journal of cellular physiology. 2018; 234(6):7885-92. doi:10.1002/jcp.27909.
11. He W-t, Wan H, Hu L, Chen P, Wang X, Huang Z, et al. Gasdermin D is an executor of pyroptosis and required for interleukin-1β secretion. Cell research. 2015; 25(12):1285-98. doi:10.1038/cr.2015.139.
12. Strowig T, Henao-Mejia J, Elinav E, Flavell R. Inflammasomes in health and disease. Nature. 2012; 481(7381):278-86. doi:10.1038/nature10759.
13. Wang S-L, Zhao G, Zhu W, Dong X-M, Liu T, Li Y-Y, et al. Herpes simplex virus-1 infection or Simian virus 40-mediated immortalization of corneal cells causes permanent translocation of NLRP3 to the nuclei. International journal of ophthalmology. 2015; 8(1):46
14. Ding J, Wang K, Liu W, She Y, Sun Q, Shi J, et al. Pore-forming activity and structural autoinhibition of the gasdermin family. Nature. 2016; 535(7610):111-6. doi:10.1038/nature18590.
15. Shi J, Zhao Y, Wang Y, Gao W, Ding J, Li P, et al. Inflammatory caspases are innate immune receptors for intracellular LPS. Nature. 2014; 514(7521):187-92. doi:10.1038/nature13683.
16. Shi J, Gao W, Shao F. Pyroptosis: Gasdermin-Mediated Programmed Necrotic Cell Death. Trends in Biochemical Sciences. 2017; 42(4):245-54. doi:10.1016/j.tibs.2016.10.004.
17. Liu X, Zhang Z, Ruan J, Pan Y, Magupalli VG, Wu H, et al. Inflammasome-activated gasdermin D causes pyroptosis by forming membrane pores. Nature. 2016; 535(7610):153-8. doi:10.1038/nature18629.

418 18. Lin J, Li D. Pyroptosis: a caspase-1-dependentcelldeath. Int J Immunol. 2011;
419 34(3):213-6
420 19. Zychlinsky A, Prevost MC, Sansonetti PJ. Shigella flexneri induces apoptosis in infected
421 macrophages. Nature. 1992; 358(6382):167-9. doi:10.1038/358167a0.
422 20. Chen LM, Kaniga K, Galán JE. Salmonella spp. are cytotoxic for cultured macrophages.
423 Molecular Microbiology. 1996; 21(5):1101-15. doi:10.1046/j.1365-2958.1996.471410.x.
424 21. Brennan MA, Cookson BT. Salmonella induces macrophage death by
425 caspase-1-dependent necrosis. Molecular Microbiology. 2000; 38(1):31-40.
426 doi:10.1046/j.1365-2958.2000.02103.x.
427 22. Watson PR, Gautier AV, Paulin SM, Bland AP, Jones PW, Wallis TS. Salmonella enterica
428 serovars Typhimurium and Dublin can lyse macrophages by a mechanism distinct from
429 apoptosis. Infect Immun. 2000; 68(6):3744-7. doi:10.1128/iai.68.6.3744-3747.2000.
430 23. Miao EA, Leaf IA, Treuting PM, Mao DP, Dors M, Sarkar A, et al. Caspase-1-induced
431 pyroptosis is an innate immune effector mechanism against intracellular bacteria. Nature
432 immunology. 2010; 11(12):1136-42. doi:10.1038/ni.1960.
433 24. Lu S, Lian L. The relationship between serum amylase polymorphism and reproductive
434 performance in Saba pig. Animal Husbandry & Veterinary Medicine. 1999(02):4-6
435 25. Vande Walle L, Lamkanfi M. Pyroptosis. Curr Biol. 2016; 26(13):R568-R72.
436 doi:10.1016/j.cub.2016.02.019.
437 26. Lamkanfi M, Dixit VM. Manipulation of Host Cell Death Pathways during Microbial
438 Infections. Cell Host Microbe. 2010; 8(1):44-54. doi:10.1016/j.chom.2010.06.007.
439 27. Wree A, Eguchi A, McGeough MD, Pena CA, Johnson CD, Canbay A, et al. NLRP3
440 inflammasome activation results in hepatocyte pyroptosis, liver inflammation, and
441 fibrosis in mice. Hepatology (Baltimore, Md). 2014; 59(3):898-910.
442 doi:10.1002/hep.26592.

443 28. Fink SL, Cookson BT. Pyroptosis and host cell death responses during Salmonella
444 infection. Cell Microbiol. 2007; 9(11):2562-70. doi:10.1111/j.1462-5822.2007.01036.x.
445 29. Cervantes J, Nagata T, Uchijima M, Shibata K, Koide Y. Intracytosolic Listeria
446 monocytogenes induces cell death through caspase-1 activation in murine macrophages.
447 Cell Microbiol. 2007; 0(0):070729204019001-???
448 doi:10.1111/j.1462-5822.2007.01012.x.
449 30. Muruve DA, Pétrilli V, Zaiss AK, White LR, Clark SA, Ross PJ, et al. The
450 inflammasome recognizes cytosolic microbial and host DNA and triggers an innate
451 immune response. Nature. 2008; 452(7183):103-7. doi:10.1038/nature06664.
452 31. Lamkanfi M, Malireddi RKS, Kanneganti T-D. Fungal zymosan and mannan activate the
453 cryopyrin inflammasome. The Journal of biological chemistry. 2009; 284(31):20574-81.
454 doi:10.1074/jbc.M109.023689.
455 32. Liang W, Ma X, Wang X. Effect of Huayu Jiedu Recipe on the Expressions of NLRP3,
456 Caspase1, and IL-1β in Kidneys of Obstructive Nephropathy Rats. Chinese Journal of
457 Integrated Traditional and Western Medicine. 2017; 37(04):470-5
458 33. Li X, He Y, Liu S. Helicobacter pylori induces cytokines IL-1β and IL-18 production in
459 human monocytic cell line through activation of NLRP3 inflammasome via ROS
460 signalingpathway. Chinese Journal of Immunology. 2015; 31(03):308-13
461 34. Ritter JL, Genco CA. Neisseria gonorrhoeae-Induced Inflammatory Pyroptosis in
462 Human Macrophages is Dependent on Intracellular Gonococci and Lipooligosaccharide.
463 J Cell Death. 2018; 11:1179066017750902-. doi:10.1177/1179066017750902.
464 35. Hutton HL, Ooi JD, Holdsworth SR, Kitching AR. The NLRP3 inflammasome in kidney
465 disease and autoimmunity. Nephrology. 2016; 21(9):736-44. doi:10.1111/nep.12785.
466 36. Hitzler I, Sayi A, Kohler E, Engler DB, Koch KN, Hardt W-D, et al. Caspase-1 Has
467 Both Proinflammatory and Regulatory Properties in Helicobacter Infections, Which Are

Differentially Mediated by Its Substrates IL-1β and IL-18. The Journal of Immunology. 2012; 188(8):3594-602. doi:10.4049/jimmunol.1103212.

37. Wei H, Li C, Liang Y. Metformin enhances ATP-stimulated inflammasome activation in LPS-primed peritoneal macrophages. Chinese Pharmacological Bulletin. 2017; 33(4):474-9

38. Liu C, Shan C, Dong Q, Fu G, Zhao R, Yan Y, et al. Pathogenic E. coli HPI upregulate the expression of inflammatory factors in porcine small intestinal epithelial cells by ubiquitin proteasome pathway. Research in Veterinary Science. 2018; 120:41-6. doi:10.1016/j.rvsc.2018.08.009.

39. Jing L, Gao F, Shan C. Investigation of HPI gene and drug resistance analysis of piglets Escherichia coli in large-scale pig farms in Chuxiong, Yunnan province. China Animal Husbandry & Veterinary Medicine. 2019; 46:1849-55

Tables

Table 1 Specific primers for amplification of target genes and β-actin gene

Name	Sequences	Primer Length	Tm (℃)	Size (bp)
β-actin	5'-TGCGGGACATCAAGGAGA-3' (F)	18	55	175
AY550069.1	5'-AGGAAGGAGGGCGGAAGAG-3' (R)	20		
NLRP3	5'-TGGATAGCGGCAAGAGT-3' (F)	17	47	145
JQ219660.1	5'-GCAGCCAGTGAGCAGAG-3' (R)	17		
Caspase-1	5'-GCCTTGCCCTCATAATCT-3' (F)	18	60	282
NM_214162.1	5'-ACATCTGGGACTTCTTCG-3' (R)	18		
IL-18	5'-GGATATGCCTGATTCTGACTGTT-3' (F)	19	50	100
AY450287.1	5'-GATGGTTACTGCCAGACCTCTA-3' (R)	19		
IL-1β	5'-GCAGTGGAGAAGCCGATGA-3' (F)	19	62	223
NM_214055.1	5'-GGTGGAGAGCCTTCAGCAT-3' (R)	19		

Figure captions

Fig. 1 A: Isolation of pathogenic *E. coli*; B: Purification of pathogenic *E. coli*; C: Microscopic examination of pathogenic *E. coli* (1,000′ magnification) D: The PCR amplification of HPI *irp2* gene (M: DL2000 Mark; 1–6: Experimental strains; 7: Negative control)

Fig. 2 The determination of IC50 for LPS

Fig. 3 A: TUNEL staining of mononuclear macrophages at different time-points after *E. coli* infection (200× magnification; TUNEL staining, green); B: The IOD value of TUNEL in mononuclear macrophages at 0.5 h, 3 h and 9 h after infection with *E. coli* HPI. **P* < 0.05, ***P* < 0.01.

Fig. 4 A: Propidium iodide (PI) staining of mononuclear macrophages after *E. coli* infection (200′, PI staining, red); B: The IOD value of PI in mononuclear macrophages at 0.5 h, 3 h and 9 h after infection with *E. coli* HPI. **P* < 0.05, ***P* < 0.01.

Fig. 5 Relative mRNA expression of NLRP3, caspase-1, IL-1β and IL-18 in mononuclear macrophages at each time-point after *E. coli* HPI infection. **P* < 0.05, ***P* < 0.01.

Fig. 6 A: Caspase-1 protein expression in mononuclear macrophages at different-point after treatment (200× magnification; caspase-1 staining, green and nuclear staining, blue); B: The IOD value of caspase-1 protein in mononuclear macrophages at 0.5 h, 3 h and 9 h after infection with *E. coli* HPI. **P* < 0.05, ***P* < 0.01.

Fig. 7 The concentration of IL-1β (A) and IL-18 (B) in mononuclear macrophages at 0.5, 3, 6, 9, 12 and 24 h after infection with *E. coli.* **P* < 0.05, ***P* < 0.01.

Figures

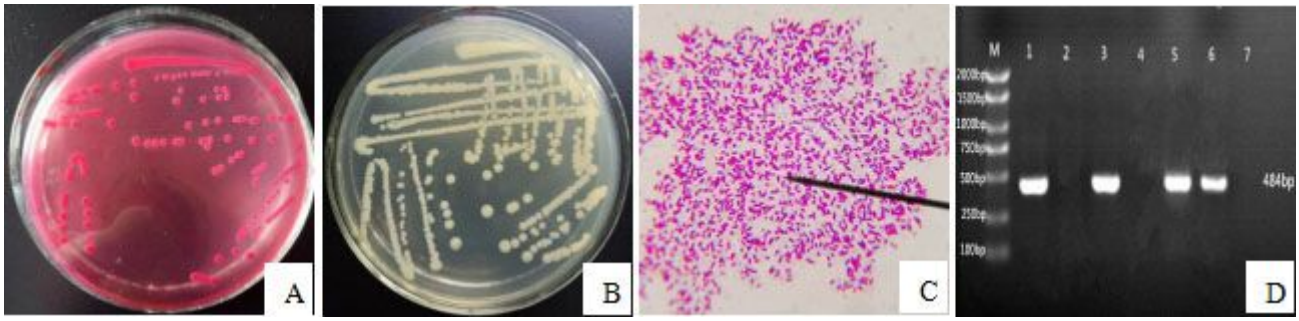

Figure 1

A: Isolation of pathogenic E. coli; B: Purification of pathogenic E. coli; C: Microscopic examination of pathogenic E. coli (1,000´ magnification) D: The PCR amplification of HPI irp2 gene (M: DL2000 Mark; 1–6: Experimental strains; 7: Negative control)

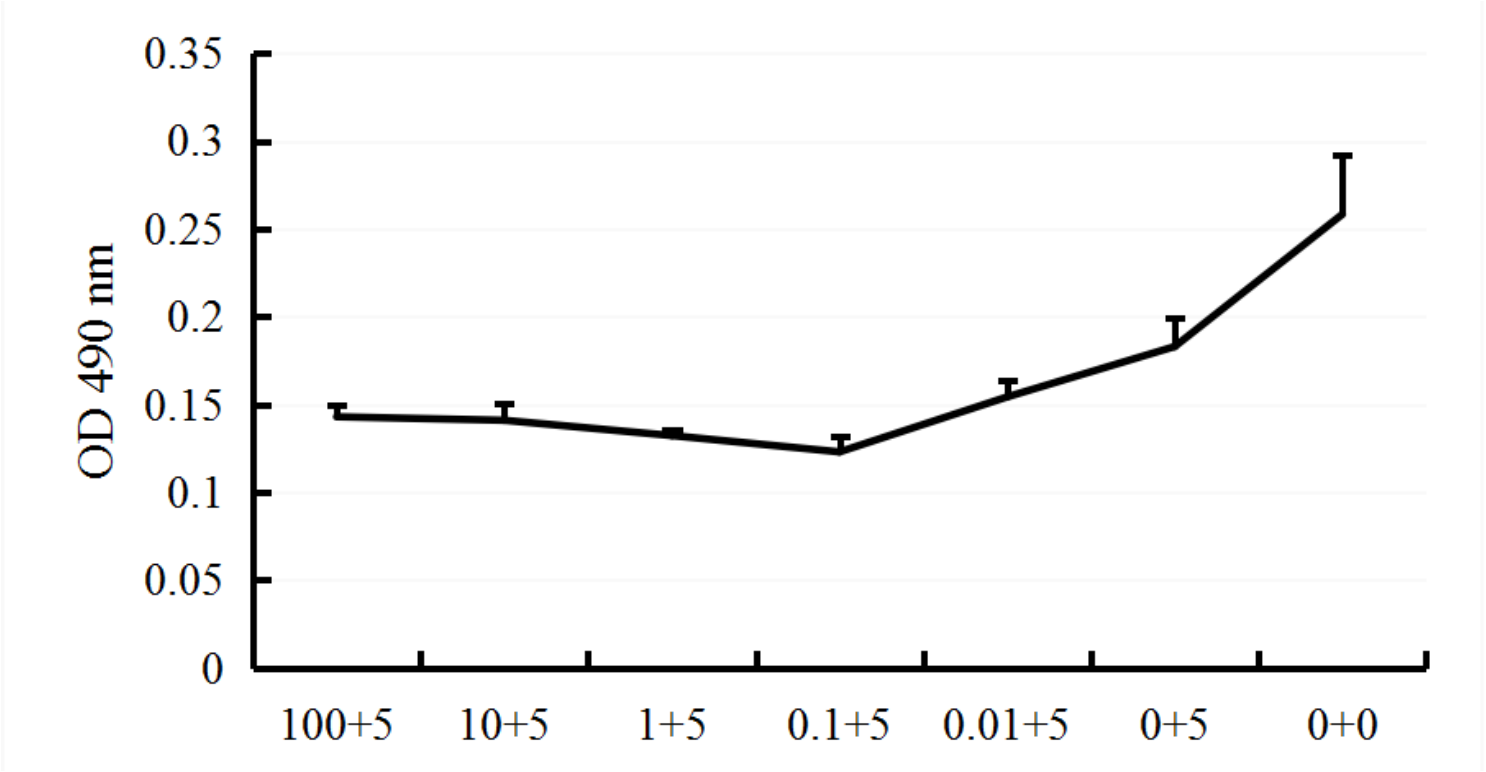

Figure 2

The determination of IC50 for LPS

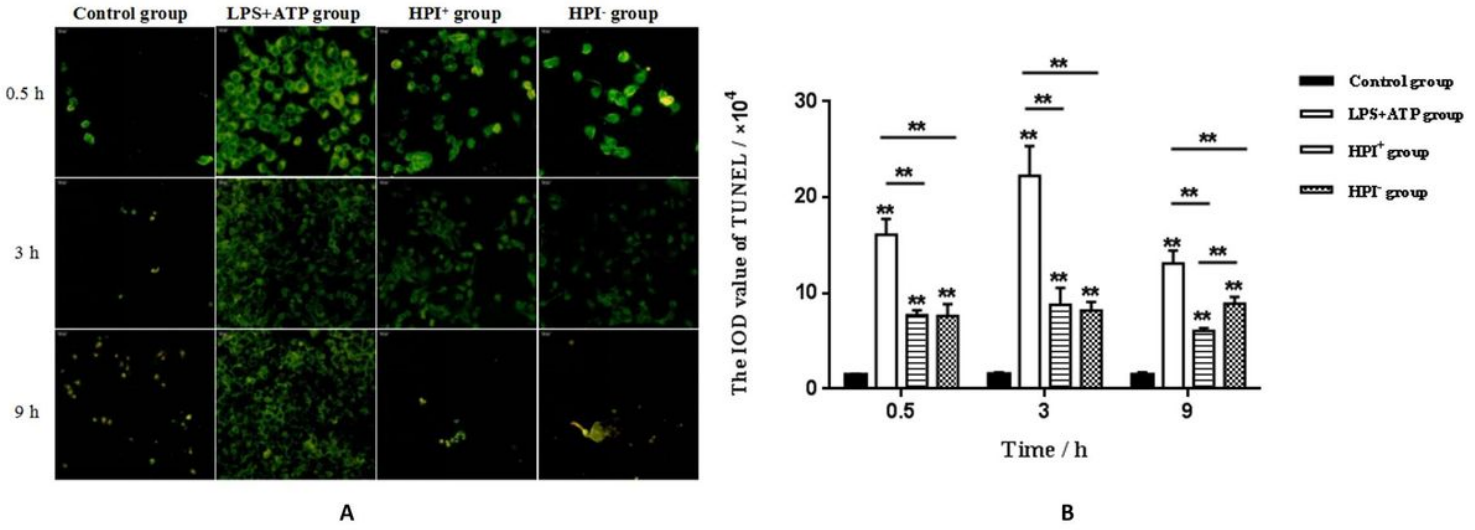

Figure 3

A: TUNEL staining of mononuclear macrophages at different time-points after E. coli infection (200× magnification; TUNEL staining, green); B: The IOD value of TUNEL in mononuclear macrophages at 0.5 h, 3 h and 9 h after infection with E. coli HPI. *P < 0.05, **P < 0.01.

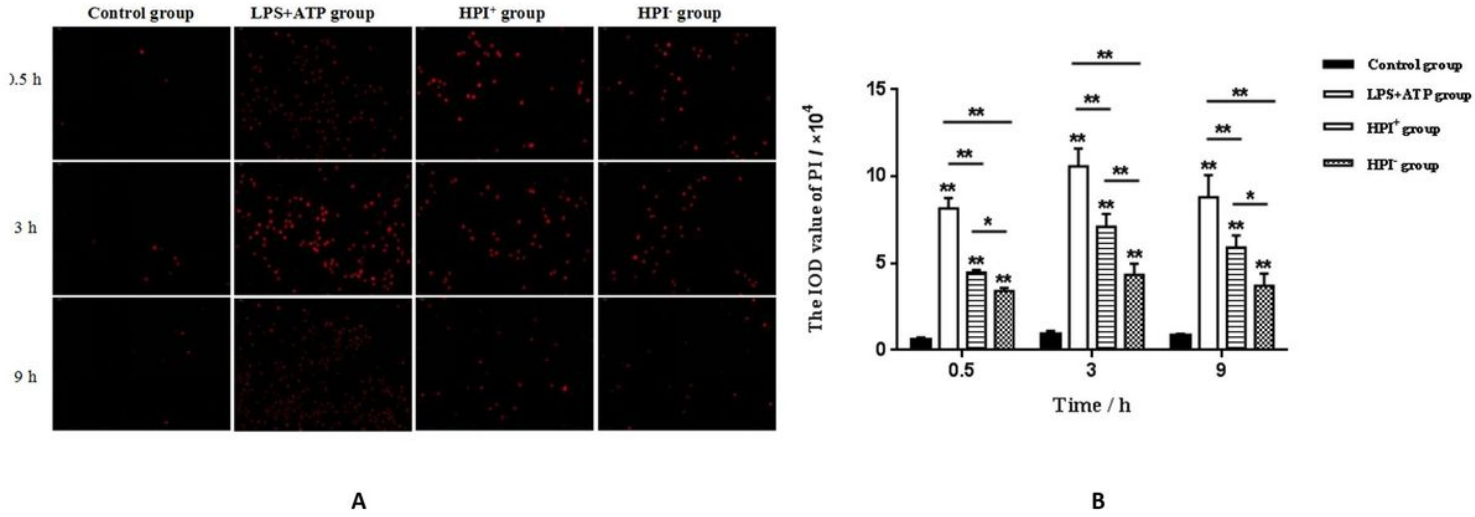

Figure 4

A: Propidium iodide (PI) staining of mononuclear macrophages after E. coli infection (200´, PI staining, red); B: The IOD value of PI in mononuclear macrophages at 0.5 h, 3 h and 9 h after infection with E. coli HPI. *P < 0.05, **P < 0.01.

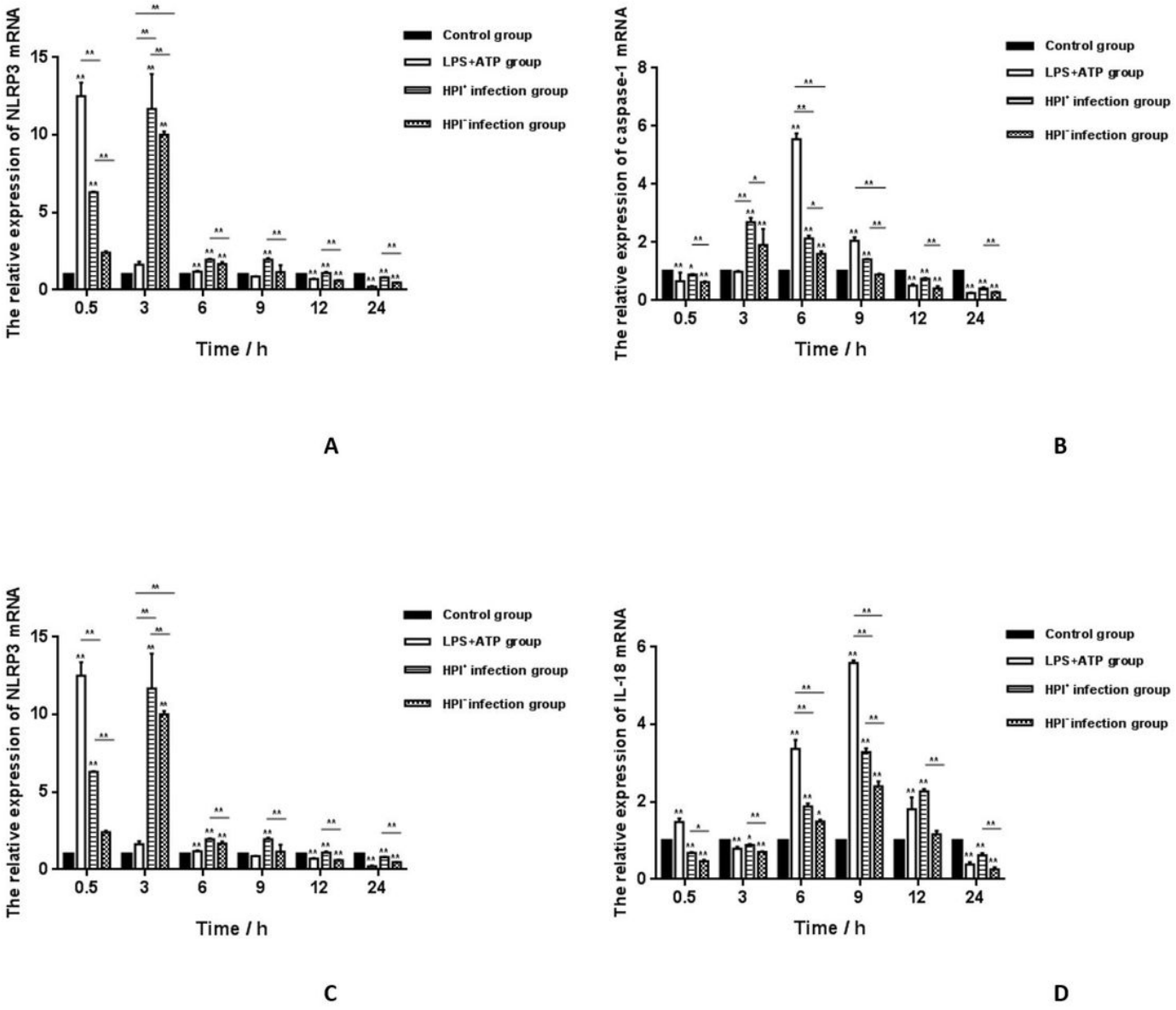

Figure 5

Relative mRNA expression of NLRP3, caspase-1, IL-1β and IL-18 in mononuclear macrophages at each time-point after E. coli HPI infection. *P < 0.05, **P < 0.01.

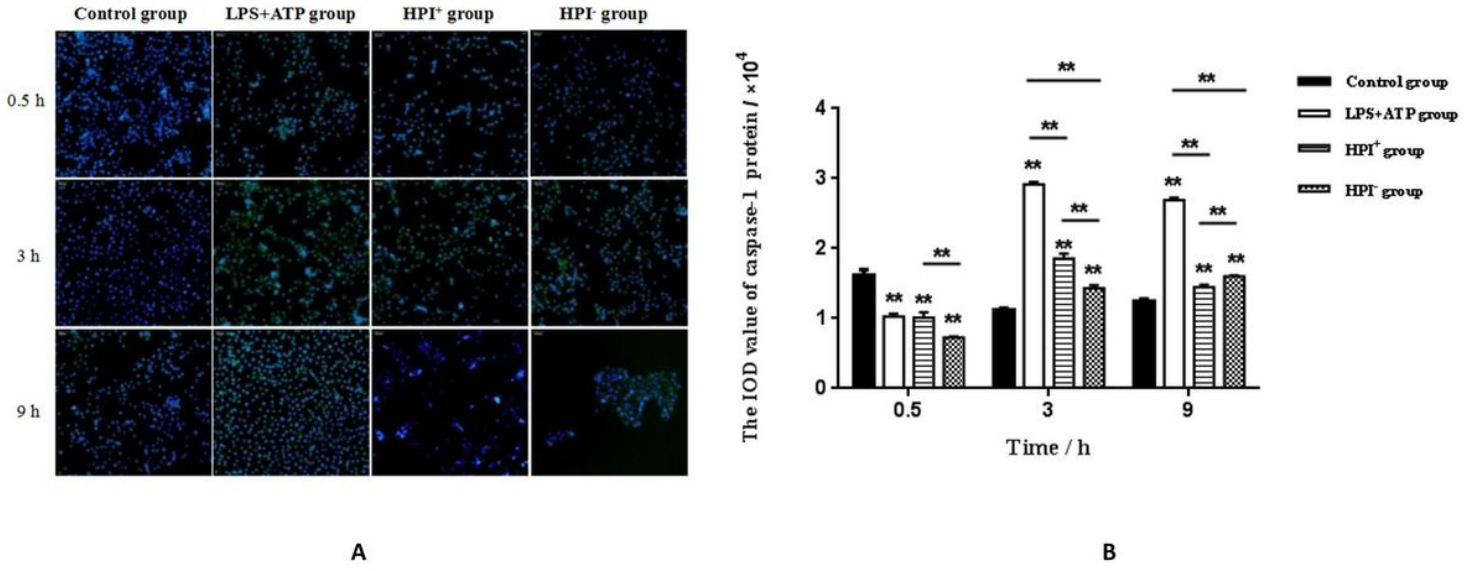

Figure 6

A: Caspase-1 protein expression in mononuclear macrophages at different-point after treatment (200× magnification; caspase-1 staining, green and nuclear staining, blue); B: The IOD value of caspase-1 protein in mononuclear macrophages at 0.5 h, 3 h and 9 h after infection with E. coli HPI. *P < 0.05, **P < 0.01.

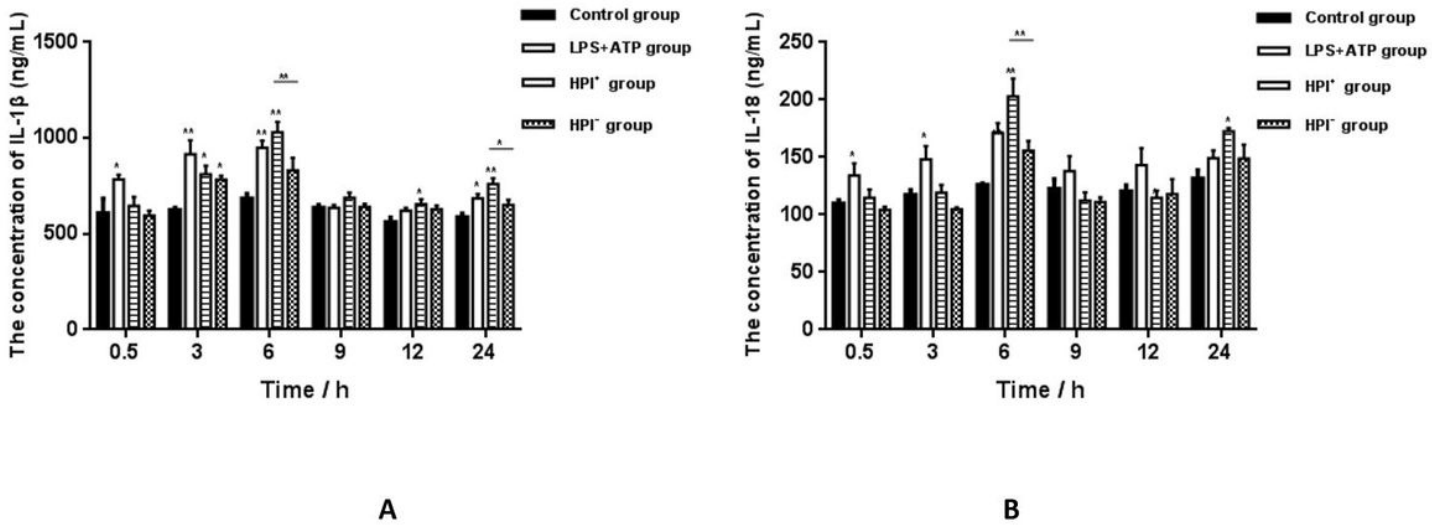

Figure 7

The concentration of IL-1β (A) and IL-18 (B) in mononuclear macrophages at 0.5, 3, 6, 9, 12 and 24 h after infection with E. coli. *P < 0.05, **P < 0.01.

Supplementary Files

This is a list of supplementary files associated with this preprint. Click to download.

- SCLFrontiersinZoologyHighlights.doc